

# Probing the interaction between dark energy and dark matter with future fast radio burst observations

Ze-Wei Zhao,<sup>a</sup> Ling-Feng Wang,<sup>a</sup> Ji-Guo Zhang,<sup>a</sup> Jing-Fei Zhang<sup>a</sup>  
and Xin Zhang<sup>a,b,c,1</sup>

<sup>a</sup>Key Laboratory of Cosmology and Astrophysics (Liaoning) & Department of Physics, College of Sciences, Northeastern University, Shenyang 110819, China

<sup>b</sup>Key Laboratory of Data Analytics and Optimization for Smart Industry (Ministry of Education), Northeastern University, Shenyang 110819, China

<sup>c</sup>National Frontiers Science Center for Industrial Intelligence and Systems Optimization, Northeastern University, Shenyang 110819, China

E-mail: [zhaozw@stumail.neu.edu.cn](mailto:zhaozw@stumail.neu.edu.cn), [lingfengwang@stumail.neu.edu.cn](mailto:lingfengwang@stumail.neu.edu.cn),  
[zhangjiguo@stumail.neu.edu.cn](mailto:zhangjiguo@stumail.neu.edu.cn), [jfzhang@mail.neu.edu.cn](mailto:jfzhang@mail.neu.edu.cn),  
[zhangxin@mail.neu.edu.cn](mailto:zhangxin@mail.neu.edu.cn)

**Abstract.** Interacting dark energy (IDE) scenario assumes that there exists a direct interaction between dark energy and cold dark matter, but this interaction is hard to be tightly constrained by the current data. Fast radio bursts (FRBs) will be seen in large numbers by future radio telescopes, and thus they have potential to become a promising low-redshift cosmological probe. In this work, we investigate the capability of future FRBs of constraining the dimensionless coupling parameter  $\beta$  in four phenomenological IDE models. If we fix the FRB properties, about  $10^5$  FRB data can give constraints on  $\beta$  tighter than the current cosmic microwave background data in the IDE models with the interaction proportional to the energy density of dark energy. In all the IDE models, about  $10^6$  FRB data can achieve the absolute errors of  $\beta$  to less than 0.10, providing a way to precisely measure  $\beta$  by only one cosmological probe. Jointly constraining the FRB properties and cosmological parameters would increase the constraint errors of  $\beta$  by a factor of about 0.5–2.

---

<sup>1</sup>Corresponding author.

---

## Contents

<b>1</b>	<b>Introduction</b>	<b>1</b>
<b>2</b>	<b>Methods and data</b>	<b>2</b>
2.1	Brief description of the IDE models	2
2.2	Mock FRB data	3
2.3	Cosmological data	5
<b>3</b>	<b>Results and discussion</b>	<b>5</b>
3.1	Constraining cosmological parameters	5
3.2	Jointly constraining cosmological parameters and DM parameters	9
<b>4</b>	<b>Conclusion</b>	<b>12</b>

---

## 1 Introduction

Fast radio bursts (FRBs) are a class of astronomical radio pulses with high energy. An FRB could interact with free electrons in the plasma and generate dispersion, resulting in its lower frequency signal being delayed. The amount of dispersion is determined by the free electron number density along the line of sight and can be quantified by dispersion measure (DM). Observed FRBs all have high DMs, exceeding the contribution from the Milky Way. This fact indicates that most FRBs are likely of extragalactic origin, except that one FRB event has been detected within the Milky Way [1, 2]. The value of DM contains the baryonic and distance information along the FRB signal’s path, so we can measure cosmological parameters by the Macquart relation, which describes the relationship between DM and redshift  $z$  [3]. A lot of works have proposed that the FRB data can constrain cosmological parameters [4–18] and related parameters [19–24]. Recent reviews and other cosmological applications can refer to refs. [25–28] and references therein.

So far, hundreds of FRB events have been detected, with more than 600 events reported by the Canadian Hydrogen Intensity Mapping Experiment (CHIME)/FRB project [29], but only a few events are localized to known host galaxies and with certain redshifts. As a result, current researches about using FRBs to measure cosmological parameters mainly focus on constraining the cosmic baryon density and the Hubble constant  $H_0$  in the base  $\Lambda$  cold dark matter ( $\Lambda$ CDM) model. Macquart et al. [3] used five localized FRBs observed by the Australian Square Kilometre Array Pathfinder (ASKAP) to derive the constraint on the cosmic baryon density with a precision of around 40%, which is consistent with the result from the big bang nucleosynthesis and the cosmic microwave background (CMB) measurements. For measuring  $H_0$  using FRBs, several independent groups [30–34] used different methods and obtained the constraints which are consistent at the  $1\sigma$  confidence level.

However, for the dark energy parameters in the extended  $\Lambda$ CDM models, current few localized FRB events cannot provide tight constraints. There is no doubt that much more localized FRBs will be detected in the future. The construction of CHIME Outrigger telescopes<sup>1</sup> and the Commensal Real-time ASKAP Fast Transients Coherent upgrade project<sup>2</sup>

---

<sup>1</sup><https://chime-experiment.ca/en>

<sup>2</sup><https://www.atnf.csiro.au/projects/askap/index.html>

are in progress and the Square Kilometre Array (SKA) project is also in construction. It is predicted that about  $10^3$ – $10^6$  FRB data could be accumulated in several years by these telescopes [25]. Previous works forecast that for the  $w$ CDM and Chevallier–Polarski–Linder (CPL) models, about  $10^4$  localized FRBs can constrain the dark energy parameters with the same precision as the CMB data [35], while for the holographic dark energy and Ricci dark energy models, more than  $10^4$  localized FRBs are needed [36].

These works show that FRBs are a promising probe to constrain dark energy parameters, but they mainly focus on the properties of dark energy and only study how the FRB data can constrain the equation of state (EoS) of dark energy. In fact, dark energy may have a direct interaction with cold dark matter, which can be described by the interacting dark energy (IDE) models (see, e.g., ref. [37] for a recent review). The IDE models could help resolve some theoretical and observational problems, such as the cosmic coincidence problem [38–42] and the  $H_0$  tension [43–50]. Because the microscopic nature of dark energy and dark matter is still unclear, the energy transfer rate in the IDE models can be considered in a purely phenomenological way [51–62], i.e., proportional to the energy density of dark energy, dark matter, or some mixture of them, and the proportionality coefficient is commonly considered as  $\beta H$  or  $\beta H_0$ . Here,  $\beta$  is a dimensionless coupling parameter [63, 64] and  $H$  is the Hubble parameter.

One can use cosmological data to constrain the parameter  $\beta$  in the IDE models to indirectly detect the interaction between dark sectors [65–81]. However, current observational data cannot precisely constrain  $\beta$  [82–85]. This is because the interaction between dark sectors mainly affects the evolution of the late-time Universe, but the current late-Universe cosmological probes are not precise enough. Measuring this interaction could deepen our understanding of dark energy and dark matter. Therefore, it is necessary to find and evaluate new late-Universe cosmological probes by using mock data. Now that FRBs have displayed fine capability on constraining dark energy parameters in some dark energy models, they may also help constrain the coupling parameter  $\beta$  in the IDE models. To study how many localized FRBs could provide precise measurement on  $\beta$ , in this paper, we simulate future FRB data to constrain four typical IDE models.

Our paper is organized as follows. In Section 2, we briefly describe the IDE models and the methods of simulating the FRB data. The constraints and relevant discussion are given in Section 3. Conclusion is given in Section 4. Throughout this paper, we adopt the units in which the speed of light equals 1.

## 2 Methods and data

### 2.1 Brief description of the IDE models

In a spatially flat Friedmann–Robertson–Walker universe, the Friedmann equation can be written as

$$3M_{\text{pl}}^2 H^2 = \rho_{\text{de}} + \rho_{\text{c}} + \rho_{\text{b}} + \rho_{\text{r}}, \quad (2.1)$$

where  $3M_{\text{pl}}^2 H^2$  is the critical density of the Universe and  $\rho_{\text{de}}$ ,  $\rho_{\text{c}}$ ,  $\rho_{\text{b}}$ , and  $\rho_{\text{r}}$  represent the energy densities of dark energy, cold dark matter, baryon, and radiation, respectively.

If we assume that there exists a direct interaction between dark energy and cold dark matter, we can obtain the energy conservation equations,

$$\dot{\rho}_{\text{de}} + 3H(1+w)\rho_{\text{de}} = Q, \quad (2.2)$$

$$\dot{\rho}_{\text{c}} + 3H\rho_{\text{c}} = -Q, \quad (2.3)$$

where the dot denotes the derivative with respect to the cosmic time  $t$ ,  $w$  is the EoS of dark energy, and  $Q$  is the energy transfer rate.

We consider the forms of  $Q$  in a purely phenomenological way and choose four typical forms, i.e.,  $Q = \beta H \rho_c$  (IDE1),  $Q = \beta H_0 \rho_c$  (IDE2),  $Q = \beta H \rho_{\text{de}}$  (IDE3), and  $Q = \beta H_0 \rho_{\text{de}}$  (IDE4). Here  $\beta > 0$  indicates cold dark matter decaying into dark energy, and  $\beta < 0$  indicates dark energy decaying into cold dark matter.  $\beta = 0$  indicates no interaction between dark energy and cold dark matter. Because we focus on how the FRB data could constrain  $\beta$ , we do not wish to introduce more extra parameters, and thus for the EoS of dark energy, we only consider  $w = -1$  (corresponding to the vacuum energy).

In the IDE models, since vacuum energy is not a true background, we need to consider the perturbations of vacuum energy. In the standard linear perturbation theory, dark energy is considered as a nonadiabatic fluid with negative pressure. Once dark energy interacts with cold dark matter, the interaction would affect the nonadiabatic pressure perturbation of dark energy and further make the nonadiabatic curvature perturbation occasionally diverge on the large scales, known as the large-scale instability problem [86–88]. To avoid this problem, one needs to use a proper approach to treat the perturbations of dark energy. In 2014, Li, Zhang, and Zhang [59, 60] extended the parametrized post-Friedmann (PPF) approach [89, 90] to the IDE models, referred to as the ePPF approach. This approach can successfully avoid the large-scale instability problem in the IDE models. In this work, we employ the ePPF method to treat the cosmological perturbations; see, e.g., refs. [91, 92] for more applications of the ePPF method.

## 2.2 Mock FRB data

The DM of an FRB can be measured by the time delay of the signal between the highest frequency and the lowest frequency. The value of DM equals the integral of the electron number density  $n_e$  weighted by  $(1+z)^{-1}$ , along the path to this FRB,

$$\text{DM} = \int \frac{n_e(l)}{1+z} dl. \quad (2.4)$$

The observed DM of an FRB can be modelled by the sum of the contributions from the Milky Way’s interstellar medium and halo, the intergalactic medium (IGM), and the FRB host galaxy,

$$\text{DM} = \text{DM}_{\text{ISM}} + \text{DM}_{\text{halo}} + \text{DM}_{\text{IGM}} + \text{DM}_{\text{host}}. \quad (2.5)$$

The average value of the cosmic contribution  $\text{DM}_{\text{IGM}}$  is expressed as

$$\langle \text{DM}_{\text{IGM}} \rangle = \frac{3H_0 \Omega_b f_{\text{IGM}}}{8\pi G m_p} \int_0^z \frac{\chi(z')(1+z') dz'}{E(z')}, \quad (2.6)$$

with

$$\chi(z) = Y_{\text{H}} \chi_{\text{e,H}}(z) + \frac{1}{2} Y_{\text{He}} \chi_{\text{e,He}}(z), \quad (2.7)$$

where  $f_{\text{IGM}} \simeq 0.83$  is the fraction of baryon mass in the IGM [93],  $\Omega_b$  is the present-day baryon fractional density,  $G$  is Newton’s constant,  $m_p$  is the proton mass,  $Y_{\text{H}} = 3/4$  is the hydrogen mass fraction, and  $Y_{\text{He}} = 1/4$  is the helium mass fraction. The terms  $\chi_{\text{e,H}}$  and  $\chi_{\text{e,He}}$  are the ionization fractions for H and He, respectively. We take  $\chi_{\text{e,H}} = \chi_{\text{e,He}} = 1$  [94], since both H and He can be regarded as fully ionized within  $z < 3$ .

The distribution of baryon matter in the IGM is inhomogeneous, so for an individual FRB,  $\text{DM}_{\text{IGM}}$  is scattered from the mean value. Here we use the power-law form of the uncertainty of  $\text{DM}_{\text{IGM}}$  fitted from the results in ref. [95],

$$\sigma_{\text{IGM}}(z) = 173.8 z^{0.4} \text{ pc cm}^{-3}, \quad (2.8)$$

where the top hat model for halos' gas profile of the ionized baryons is assumed.

The value of  $\text{DM}_{\text{ISM}}$  is estimated by the NE2001 model<sup>3</sup>,  $\text{DM}_{\text{halo}}$  is set to be  $\text{DM}_{\text{halo}} = 50 \text{ pc cm}^{-3}$ , and their uncertainties can be absorbed in the uncertainty of  $\text{DM}_{\text{host}}$  [3, 32]. From eq. (2.5), we can see that if we further ignore the uncertainty of  $\text{DM}_{\text{obs}}$ , which is enough small relative to the other errors, the total uncertainty is determined by

$$\sigma_{\text{DM}} = \left[ \sigma_{\text{IGM}}^2 + \left( \frac{\sigma_{\text{host}}}{1+z} \right)^2 \right]^{1/2}. \quad (2.9)$$

Following ref. [19], we assume that the uncertainty of  $\text{DM}_{\text{host}}$  would achieve  $\sigma_{\text{host}} = 30 \text{ pc cm}^{-3}$ . If the values of  $\text{DM}_{\text{ISM}}$ ,  $\text{DM}_{\text{halo}}$ , and  $\text{DM}_{\text{host}}$  are known and we adopt the assumption that all the FRB data are independent, then the  $\chi^2$  function is simply written as

$$\chi_{\text{cos}}^2 = \sum_{i=1}^N \left[ \frac{\text{DM}_i - \langle \text{DM}_{\text{IGM}} \rangle(z_i; \boldsymbol{\theta})}{\sigma_{\text{DM}}(z_i)} \right]^2, \quad (2.10)$$

where  $z_i$  and  $\text{DM}_i$  represent the redshift and DM of the  $i$ -th mock FRB data, respectively,  $N$  is the total event number, and  $\boldsymbol{\theta}$  denotes cosmological parameters, including the six base  $\Lambda$ CDM cosmological parameters and an extra IDE parameter  $\beta$ . The Hubble constant  $H_0$  and the present-day matter density  $\Omega_m$  are derived parameters. Then we treat  $\boldsymbol{\theta}$  as free parameters and use the Markov Chain Monte Carlo (MCMC) method to constrain them. It should be noted that actually the DM values of FRB data are correlated due to long wavelength modes of the electron distribution of the large-scale structure [96]. The effect of the correlation on cosmological constraints depends on the sky area and the number of events of the observed FRB data. A more accurate calculation of the FRB likelihood should include the survey area of different telescopes and the covariance between different FRB data. We leave this study to future work.

The method above focuses on only constraining cosmological parameters and depends on some assumptions of  $\text{DM}_{\text{host}}$ , i.e., the mean value of  $\text{DM}_{\text{host}}$  is fixed to the best-fit constraint values or the values from cosmological simulations [97]. Jointly constraining the FRB properties and cosmological parameters is more realistic by considering their correlations.

For simplicity, we assume that the distribution of  $\text{DM}_{\text{host}}$  can be approximated as a Gaussian function with the fiducial mean value  $\mu_{\text{fid}} = 100 \text{ pc cm}^{-3}$  and standard deviation  $20 \text{ pc cm}^{-3}$ . According to this distribution, we randomly select a  $\text{DM}_{\text{host}}$  value for each FRB event and add it to the DM value, with the redshift correction  $1/(1+z)$ . If  $\mu$  has an intrinsic redshift evolution, we assume a power-law evolution  $\mu(z) = \mu(1+z)^\gamma$  and set  $\gamma_{\text{fid}} = 0.7$ . We model the  $\chi^2$  function as

$$\chi_{\text{joint}}^2 = \sum_{i=1}^N \left[ \frac{\text{DM}_i - \frac{\mu(1+z)^\gamma}{1+z} - \langle \text{DM}_{\text{IGM}} \rangle(z_i; \boldsymbol{\theta})}{\sigma_{\text{DM}}(z_i)} \right]^2. \quad (2.11)$$

---

<sup>3</sup>Ben Bar-Or, J. Prochaska, available at <https://readthedocs.org/projects/ne2001/>

We first assume the  $DM_{\text{host}}$  distribution does not evolve with redshift (i.e.  $\gamma = 0$ ) and treat  $\mu$  and  $\theta$  as free parameters. Then we consider the redshift evolution of  $DM_{\text{host}}$  by treating all the DM parameters (i.e.  $\mu$  and  $\gamma$ ) and cosmological parameters  $\theta$  as free parameters and use MCMC to jointly constrain them.

In the era of SKA, it is expected that  $10^5$ - $10^6$  FRBs could be detected per year [98]. Assuming that the observation duration of SKA is 10-year and 1/10 of FRBs can be localized to the host galaxy with redshift, we consider a conservative expectation with the mock FRB event number  $N_{\text{FRB}} = 10^5$  and an optimistic expectation with  $N_{\text{FRB}} = 10^6$  (a detailed discussion about the FRB event number can refer to ref. [99]).

Except for a Galactic magnetar, the progenitors of FRBs have not been generally identified. Therefore, the accurate redshift distribution of FRBs is unknown. Based on the first CHIME/FRB catalog, the common assumption that FRBs' population tracks the star formation history (SFH) of the Universe has been ruled out [100]. Qiang et al. [101] also confirmed this result, and proposed some empirical distribution models consistent with the observational data. We use the simple power-law model of redshift distribution to simulate the FRB data. The event rate of mock FRB data is

$$N_{\text{SFH}}(z) = (1+z)^\gamma \mathcal{N}_{\text{SFH}} \frac{\dot{\rho}_* d_C^2(z)}{H(z)(1+z)} e^{-d_L^2(z)/[2d_L^2(z_{\text{cut}})]}, \quad (2.12)$$

where  $(1+z)^\gamma$  represents the delay with respect to SFH with  $\gamma = -1.1$  [101],  $\mathcal{N}_{\text{SFH}}$  is a normalization factor,  $d_C$  is the comoving distance,  $d_L$  is the luminosity distance, and  $z_{\text{cut}} = 1$  is a Gaussian cutoff above which the number of detected FRBs would decrease due to the detection threshold. The form of SFH is [101, 102]

$$\dot{\rho}_*(z) = \frac{(1+z)^{2.6}}{1 + ((1+z)/3.2)^{6.2}}. \quad (2.13)$$

The statistical properties of the mock FRB data with  $N_{\text{FRB}} = 10^5$  in the fiducial IDE1 cosmology are shown in figure 1.

### 2.3 Cosmological data

For the current cosmological data as comparison, we use the *Planck* 2018 CMB “distance priors” [103], and the baryon acoustic oscillation (BAO) measurements from 6dFGS at  $z_{\text{eff}} = 0.106$  [104], SDSS-MGS at  $z_{\text{eff}} = 0.15$  [105], and BOSS-DR12 at  $z_{\text{eff}} = 0.38, 0.51,$  and  $0.61$  [106]. For the type Ia supernova (SN) data, we use the sample from the Pantheon compilation with 1048 data [107]. When we generate the mock FRB data, the fiducial values of cosmological parameters are taken to be the same with the CMB+BAO+SN results. We use the modified *CAMB* [108] and *cosmomc* codes [109] with the inclusion of the ePPF module and obtain the posterior probability distribution of cosmological parameters.

## 3 Results and discussion

### 3.1 Constraining cosmological parameters

In this section, we study the capability of the mock FRB data of constraining the parameters in the IDE models, with fixed DM parameters. The  $1\sigma$  errors of cosmological parameters are listed in table 1. We use FRB1 and FRB2 to denote the mock FRB data in the conservative

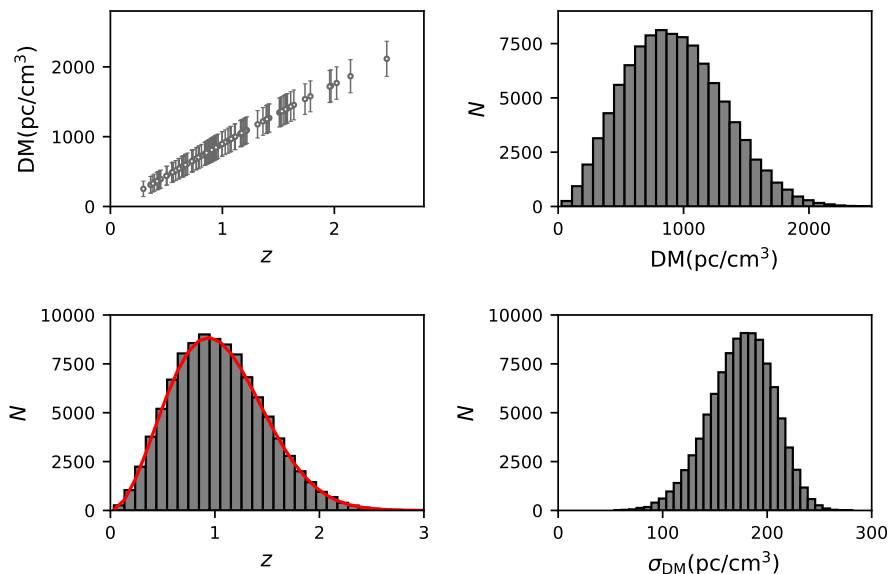


**Figure 1.** The statistical properties of mock FRB data with  $N_{\text{FRB}} = 10^5$  in the fiducial IDE1 cosmology. Top left panel: the representative FRB events with  $1\sigma$  errors. We show one data point for every 1000 events. Top right panel: The histogram of FRB event number versus DM. Bottom left panel: The redshift evolution of FRB event number. The assumed probability distribution function of redshift is also shown by solid red line. Bottom right panel: The histogram of FRB event number versus  $\sigma_{\text{DM}}$ .

expectation case (i.e.,  $N_{\text{FRB}} = 10^5$ ) and the optimistic expectation case (i.e.,  $N_{\text{FRB}} = 10^6$ ), respectively.

First, in all the IDE models, about  $10^6$  FRB data can constrain  $\beta$  to less than 0.10. We show the constraints from the FRB2 data in each IDE model in figure 2. Future FRBs provide a way to precisely measure  $\beta$  by using only one cosmological probe. In the following, we will discuss the constraints on  $\beta$  in each IDE model in sequence. For the IDE1 model ( $Q \propto \beta H \rho_c$ ), the CMB data alone can tightly constrain  $\beta$ , because  $H \rho_c$  is sensitive to the early-universe probes. The constraint on  $\beta$  from the CMB data,  $\sigma(\beta) = 0.0025$ , is even tighter by an order of magnitude than the one from the FRB2 data,  $\sigma(\beta) = 0.023$ . Nevertheless, the combined analysis could still improve the constraint. The CMB+FRB1 data could give  $\sigma(\beta) = 0.00084$ , and the CMB+BAO+SN+FRB2 data could give  $\sigma(\beta) = 0.00051$ . The addition of FRB data could help constrain the absolute error of  $\beta$  to achieve less than 0.0010 in the IDE1 model.

Except for the IDE1 model, the CMB data alone cannot provide tight constraints on  $\beta$  in other IDE models. For the IDE2 model, the CMB data can give  $\sigma(\beta) = 0.22$ , and the FRB1 data can give a better constraint with  $\sigma(\beta) = 0.12$ . However, the combined constraint from CMB+FRB1 is significantly better than the result from either the CMB data or the FRB1 data alone. The CMB+FRB1 data can give  $\sigma(\beta) = 0.022$ . Compared to using the CMB data alone and the FRB1 data alone, this combination improves the constraints by about 90% and 82%, respectively. The two-dimensional marginalized posterior probability contours are shown in the left panel of figure 3, from the CMB, FRB1, and CMB+FRB1 data. The orientations of the contours in the  $\beta$ - $\Omega_m$  plane constrained by CMB and by FRB are rather

**Table 1.** Absolute errors ( $1\sigma$ ) of the cosmological parameters in each IDE model from the CMB, FRB1, CMB+FRB1, CBS, FRB2, and CBS+FRB2 data, assuming fixed DM parameters ( $\mu$  and  $\gamma$ ). FRB1 and FRB2 denote the FRB data with the event number  $N_{\text{FRB}} = 10^5$  and  $N_{\text{FRB}} = 10^6$ , respectively. Here, CBS stands for the CMB+BAO+SN data and  $H_0$  is in units of  $\text{km s}^{-1} \text{Mpc}^{-1}$ .

Model	Parameter	CMB	FRB1	CMB+FRB1	CBS	FRB2	CBS+FRB2
IDE1	$\beta$	0.0025	0.073	0.00084	0.0013	0.023	0.00051
	$H_0$	1.8	13	0.34	0.69	10	0.15
	$\Omega_{\text{m}}$	0.024	0.016	0.0043	0.0083	0.0049	0.0016
IDE2	$\beta$	0.22	0.12	0.022	0.044	0.039	0.020
	$H_0$	4.9	13	0.31	0.83	13	0.13
	$\Omega_{\text{m}}$	0.15	0.019	0.0060	0.016	0.0063	0.0037
IDE3	$\beta$	0.47	0.16	0.070	0.10	0.049	0.040
	$H_0$	4.6	13	0.40	0.83	13	0.16
	$\Omega_{\text{m}}$	0.15	0.035	0.017	0.028	0.011	0.0090
IDE4	$\beta$	0.50	0.23	0.13	0.16	0.071	0.061
	$H_0$	3.2	13	0.48	0.82	13	0.18
	$\Omega_{\text{m}}$	0.13	0.043	0.027	0.035	0.014	0.012

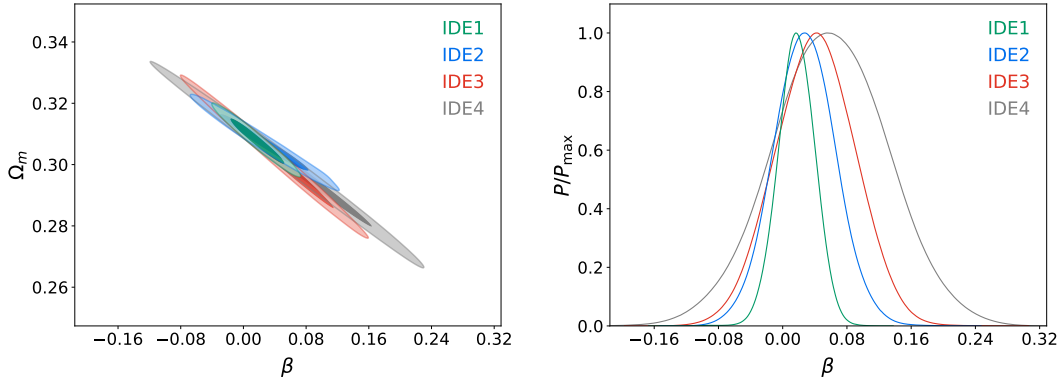


**Figure 2.** Constraints (68.3% and 95.4% confidence level) on  $\beta$  and  $\Omega_{\text{m}}$  (left panel) and one-dimensional marginalized probability distributions of  $\beta$  (right panel) from the FRB2 data, in each IDE model.

different. Combining the CMB and FRB data could break the parameter degeneracies, and thus evidently improve the constraints. This effect also exists when combining the CMB+BAO+SN and FRB2 data and we show it in the right panel of figure 3. The addition of the FRB2 data will tighten the CMB+BAO+SN constraint with the absolute error improved from  $\sigma(\beta) = 0.044$  to  $\sigma(\beta) = 0.020$ .

For the IDE3 and IDE4 models ( $Q \propto \beta \rho_{\text{de}}$ ), even the current mainstream data CMB+BAO+SN

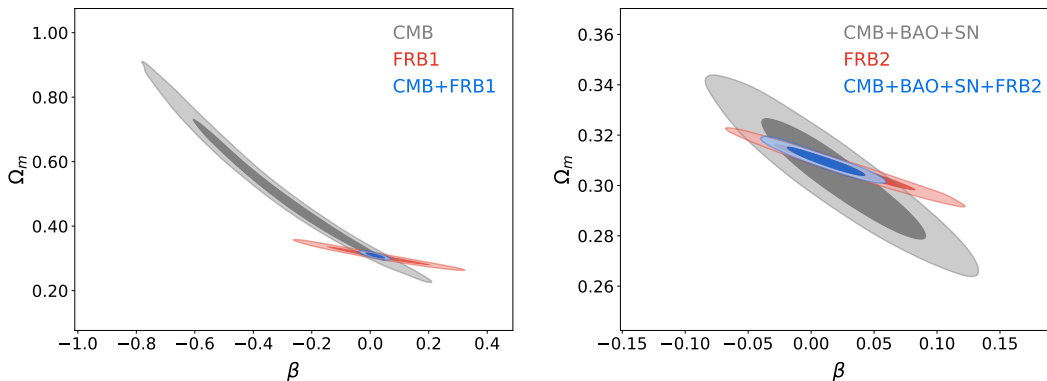


**Figure 3.** Constraints (68.3% and 95.4% confidence level) on  $\beta$  and  $\Omega_m$  in the IDE2 model with  $Q = \beta H_0 \rho_c$  from the CMB, FRB1, and CMB+FRB1 data (left panel) and from the CMB+BAO+SN, FRB2, and CMB+BAO+SN+FRB2 data (right panel).

cannot constrain the absolute errors of  $\beta$  to less than 0.10, urging a new probe to tightly constrain them. For the IDE3 model, the constraint errors on  $\beta$  from the CMB, FRB1, CMB+BAO+SN, and FRB2 data are 0.47, 0.16, 0.10, and 0.049, respectively. We plot the comparison of these constraints in the left panel of figure 4. The CMB+FRB1 data can constrain  $\beta$  to less than 0.10, with  $\sigma(\beta) = 0.070$ . The CMB+BAO+SN+FRB2 data can give constraint  $\sigma(\beta) = 0.040$ , slightly tighter than the result from the FRB2 data.

For the IDE4 model, the constraint errors of  $\beta$  from the CMB and CMB+BAO+SN data are 0.50 and 0.16, respectively, which are the worst among all the IDE models. The constraints on  $\beta$  from the FRB1 data and the FRB2 data are 0.23 and 0.071, respectively. The comparison of these constraints is shown in the right panel of figure 4. We find that, for the IDE models with  $Q$  proportional to  $\beta \rho_{de}$ , about  $10^5$  FRB data can give constraint on  $\beta$  tighter than the CMB data, but weaker than the CMB+BAO+SN data. About  $10^6$  FRB data can give constraint on  $\beta$  tighter than the CMB+BAO+SN data. This also displays the advantage of the future FRB data in constraining  $\beta$  by one probe. Similar to the results in the IDE3 model, the constraint from the CMB+BAO+SN+FRB2 data,  $\sigma(\beta) = 0.061$ , is only slightly tighter than the result from the FRB2 data. For the IDE models with  $Q$  proportional to  $\beta \rho_{de}$ , the main contribution to the  $\beta$  constraints in the combined analysis is from the FRB data.

The redshift evolutions of the interaction term  $Q(z)$  can be reconstructed by the constraints. In figure 5, we show the evolution of  $Q/(H_0 \rho_{cr0})$  versus  $z$  in the IDE1 and IDE3 models, where  $\rho_{cr0} = 3M_{pl}^2 H_0^2$  is the present-day critical density of the Universe. The best-fit line and the  $1\sigma$  region are shown in the figure. We find that in the IDE1 model, although the CMB+BAO+SN data alone can precisely constrain  $\beta$ , the addition of the FRB data could significantly shrink the uncertainty of  $Q$  in the redshift region with  $z > 3$ . In the IDE3 model, the addition of the FRB data could help constrain the evolution of  $Q$  in the whole redshift region.

We briefly discuss the constraints on  $H_0$ . The FRB data alone cannot effectively constrain  $H_0$ , since DM is proportional to  $\Omega_b H_0^2$ . However, the CMB data could provide tight constraint on  $\Omega_b H_0^2$ , resulting in tight  $H_0$  constraints if combining the CMB and FRB data. This effect can be seen in figure 6, in accordance with the previous experience in the  $w$ CDM and CPL models [35]. In all the IDE models, even the CMB+BAO+SN data cannot con-

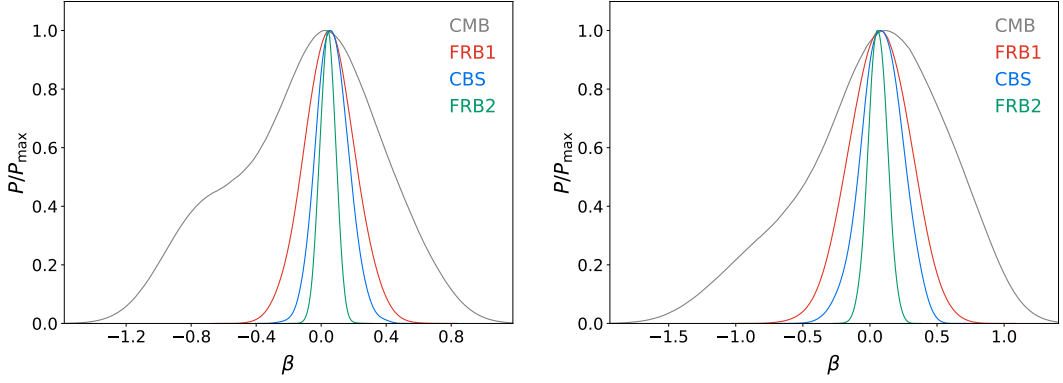


**Figure 4.** One-dimensional marginalized probability distributions of  $\beta$  in the IDE3 model with  $Q = \beta H \rho_{\text{de}}$  (left panel) and in the IDE4 model with  $Q = \beta H_0 \rho_{\text{de}}$  (right panel), from the CMB, FRB1, CMB+BAO+SN, and FRB2 data.

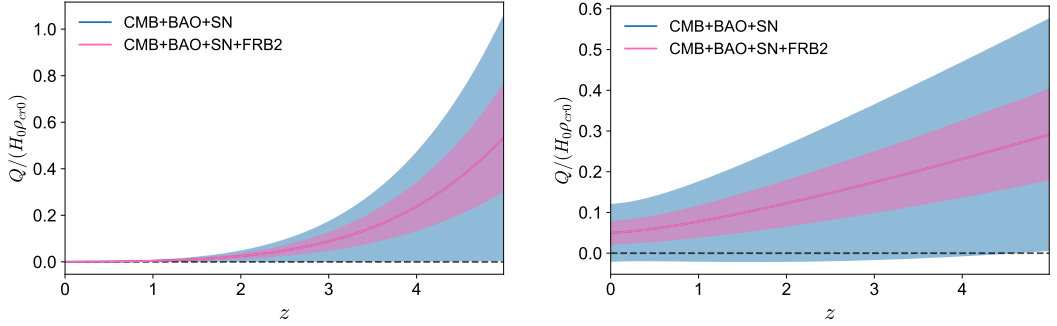


**Figure 5.** The redshift evolutions of  $Q/(H_0 \rho_{\text{cr}0})$  in the IDE1 model with  $Q = \beta H \rho_c$  (left panel) and in the IDE3 model with  $Q = \beta H \rho_{\text{de}}$  (right panel). The blue and pink shaded regions represent the  $1\sigma$  constraints from the CMB+BAO+SN and CMB+BAO+SN+FRB2 data, respectively. The black dashed lines denote the  $\Lambda$ CDM model ( $Q = 0$ ).

strain  $H_0$  at sub-percent precision, yet the CMB+FRB1 data could do. For example, in the IDE4 model, the CMB data can only provide a 4.7% measurement for  $H_0$ , while the CMB+FRB1 data can constrain  $H_0$  to a 0.71% precision. The constraint is improved by about 85%. The CMB+BAO+SN data provide a 1.2% measurement for  $H_0$ , whereas the combined CMB+BAO+SN+FRB2 data provide a 0.27% measurement.

The values of  $\sigma_{\text{host}}$  have minor effect on the cosmological constraints. We calculate two new cases for the IDE3 model assuming  $\sigma_{\text{host}} = 20 \text{ pc cm}^{-3}$  and  $\sigma_{\text{host}} = 60 \text{ pc cm}^{-3}$ . For example,  $10^6$  FRB data with  $\sigma_{\text{host}} = 60 \text{ pc cm}^{-3}$  could give  $\sigma(\beta) = 0.051$  in the IDE3 model, while  $10^6$  FRB data with  $\sigma_{\text{host}} = 20 \text{ pc cm}^{-3}$  could give  $\sigma(\beta) = 0.049$ . There are two reasons: (i) the values of  $\sigma_{\text{IGM}}$  are larger than  $\sigma_{\text{host}}$ , and (ii)  $\sigma_{\text{host}}$  contributes to the total uncertainties by multiplying a factor  $1/(1+z)$ . In figure 7, we can clearly see that  $\sigma_{\text{DM}}$  is dominated by  $\sigma_{\text{IGM}}$  except for very low redshift.

### 3.2 Jointly constraining cosmological parameters and DM parameters

We use the IDE1 and IDE3 models as examples to illustrate the effect of treating the DM parameters as free parameters. The constraints on the IDE1 and IDE3 models and the DM

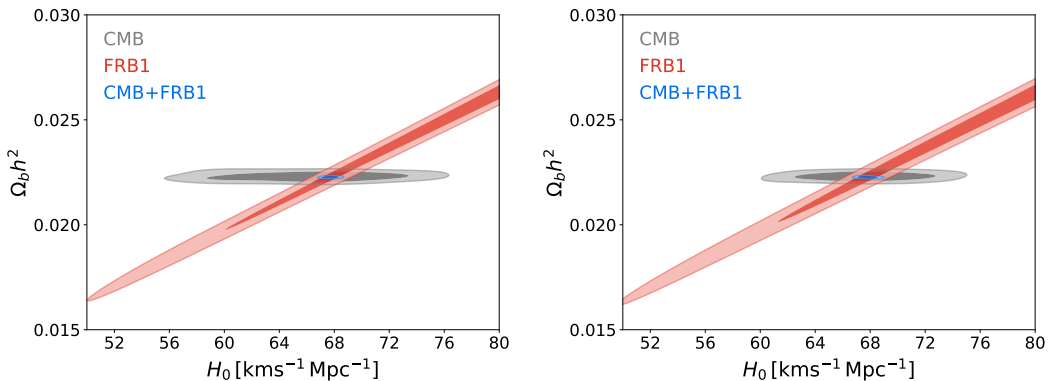


**Figure 6.** Constraints (68.3% and 95.4% confidence level) on  $H_0$  and  $\Omega_b h^2$  in the IDE3 model with  $Q = \beta H \rho_{\text{de}}$  (left panel) and the IDE4 model with  $Q = \beta H_0 \rho_{\text{de}}$  (right panel) from the CMB, FRB1, and CMB+FRB1 data.

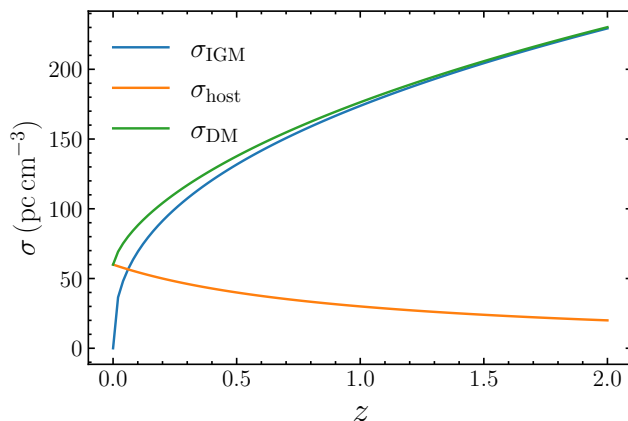


**Figure 7.** The evolutions of  $\sigma_{\text{IGM}}$ ,  $\sigma_{\text{host}}$ , and  $\sigma_{\text{DM}}$ , assuming  $\sigma_{\text{host}} = 60 \text{ pc cm}^{-3}$ .

parameters are listed in table 2. We first consider the case without  $\text{DM}_{\text{host}}$  redshift evolution (i.e.,  $\gamma = 0$ ). The constraint contours for the IDE3 model from the FRB1 and FRB2 data are shown in the left panel of figure 8, and the fiducial values are denoted by dotted lines. We can clearly see that all constraints of the DM parameters and cosmological parameters could cover their fiducial values.

Because of the correlations between  $\mu$  and cosmological parameters, treating  $\mu$  as a free parameter weakens the constraints on  $\beta$  and  $\Omega_m$  in the global fit. If  $\mu$  is free, the absolute errors of  $\beta$  are broader by about 50%, compared to the ones with fixed  $\mu$ . For example, the FRB1 data can give  $\sigma(\beta) = 0.16$  in the IDE3 model with fixed  $\mu$ , and give  $\sigma(\beta) = 0.26$  when  $\mu$  is a free parameter, which is 62.5% looser than the former constraint. The constraints of  $\beta$  from the FRB1 and FRB2 data are still comparable to the CMB and CMB+BAO+SN results, respectively. The main results do not change significantly.

For the case that  $\mu$  and  $\gamma$  both are free, the constraints on the IDE1 model are shown in the right panel of figure 8 and can also cover the fiducial values. The absolute errors of  $\beta$  are about 1–2 times broader than the ones with fixed  $\mu$  and  $\gamma$ . For example, in the IDE1 model,

**Table 2.** Constraints on the IDE1 and IDE3 models and the DM parameters from  $10^5$  mock FRB data (FRB1) and  $10^6$  mock FRB data (FRB2), with different fixed DM parameters. Here,  $\mu$  is in units of  $\text{pc cm}^{-3}$ .

Sample	DM parameter	IDE1 ( $Q = \beta H \rho_c$ )				IDE3 ( $Q = \beta H \rho_{\text{de}}$ )			
		$\sigma(\beta)$	$\sigma(\Omega_m)$	$\sigma(\mu)$	$\sigma(\gamma)$	$\sigma(\beta)$	$\sigma(\Omega_m)$	$\sigma(\mu)$	$\sigma(\gamma)$
FRB1	$\mu, \gamma$ fixed	0.073	0.016			0.16	0.035		
	$\gamma$ fixed	0.10	0.028	3.6		0.26	0.068	4.4	
	both free	0.15	0.091	4.9	1.1	0.50	0.16	5.2	1.2
FRB2	$\mu, \gamma$ fixed	0.023	0.0049			0.049	0.011		
	$\gamma$ fixed	0.033	0.0087	1.1		0.085	0.021	1.4	
	both free	0.050	0.041	1.7	0.48	0.137	0.056	1.5	0.64

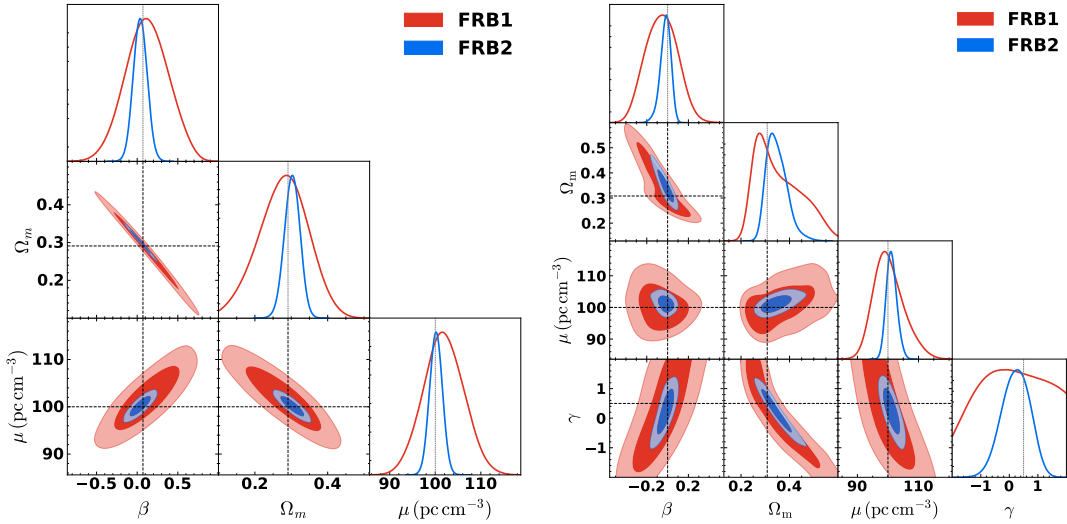


**Figure 8.** Constraints on the IDE3 model ( $Q = \beta H \rho_{\text{de}}$ ) and the mean value of  $\text{DM}_{\text{host}}$  (left panel) and the IDE1 model ( $Q = \beta H \rho_c$ ) and the mean value and redshift evolution of  $\text{DM}_{\text{host}}$  (right panel), using the FRB1 and FRB2 data. The fiducial values are denoted by dotted lines.

the constraint  $\sigma(\beta) = 0.15$  from the FRB1 data when  $\mu$  and  $\gamma$  both are free parameters is 105.5% looser than the constraint with fixed  $\mu$  and  $\gamma$ ,  $\sigma(\beta) = 0.073$ .

The constraint errors of the DM parameters are similar for different IDE models. For example, in the case of  $\gamma$  fixed, the FRB2 data could give  $\sigma(\mu) = 1.1 \text{ pc cm}^{-3}$  and  $\sigma(\mu) = 1.4 \text{ pc cm}^{-3}$  for the IDE1 model and the IDE3 model, respectively. In all the cases (i.e., in both IDE1 and IDE3 models with whether  $\gamma$  fixed or not), the FRB1 data could give  $\sigma(\mu) \sim 4.5 \text{ pc cm}^{-3}$  and the FRB2 data could give  $\sigma(\mu) \sim 1.5 \text{ pc cm}^{-3}$ . However, we note that these constraints are somewhat meaningless, because with a large number of FRB data,

the asymmetry of  $DM_{\text{host}}$  distribution would affect the constraints. Using a log-normal distribution may be more appropriate to account for observed high  $DM_{\text{host}}$  values [3, 110]. In this work, we focus on the constraints on cosmological parameters, and leave the detailed research on  $DM_{\text{host}}$  distribution to future work. The redshift evolution of  $DM_{\text{host}}$ ,  $\gamma$ , is hard to be constrained by the FRB1 data, but the FRB2 data could constrain its absolute error to about 0.60. However, we still need more data or new methods to precisely constrain it.

## 4 Conclusion

In this paper, we study how many FRBs are needed to precisely measure the interaction between dark energy and cold dark matter, by constraining  $\beta$  in the IDE models. Four phenomenological IDE models are considered, i.e.,  $Q = \beta H \rho_c$  (IDE1),  $Q = \beta H_0 \rho_c$  (IDE2),  $Q = \beta H \rho_{\text{de}}$  (IDE3), and  $Q = \beta H_0 \rho_{\text{de}}$  (IDE4). We simulate the future FRB data with data number  $N_{\text{FRB}} = 10^5$  (FRB1) and  $N_{\text{FRB}} = 10^6$  (FRB2), based on the current knowledge of FRBs from the first CHIME/FRB catalog and ASKAP.

We find that, if we fix the FRB properties, in all the IDE models, about  $10^6$  FRB data alone can constrain the absolute error of  $\beta$  to less than 0.10. This provides a way to constrain  $\beta$  by only one cosmological probe. For the IDE1 model, although the CMB data can provide tight constraint on  $\beta$ , the addition of the FRB data could still improve the constraint. The combined analysis is also important in the IDE2 model. In this model, the CMB and FRB data could obviously break the parameter degeneracies inherent in each other. Therefore, compared to the result from the CMB data or the CMB+BAO+SN data, the combined constraint on  $\beta$  is significantly improved with the addition of the FRB data.

For the IDE3 and IDE4 models with  $Q$  proportional to  $\beta \rho_{\text{de}}$ , even the current CMB+BAO+SN data cannot constrain the absolute errors of  $\beta$  to less than 0.10. We find that about  $10^5$  FRB data can give constraint on  $\beta$  tighter than the CMB data and about  $10^6$  FRB data can give constraint on  $\beta$  tighter than the CMB+BAO+SN data. In the combined analysis, the main contribution to the combined constraints is from the FRB data. As a low-redshift probe, the FRB data alone could play an important role in these models.

We reconstruct the redshift evolution of the interaction term  $Q(z)$ . The addition of the FRB data could help check whether the interaction exists at a high confidence level, and eventually provide evidence to distinguish between the  $\Lambda$ CDM model and the IDE models. With respect to the Hubble constant, the CMB+FRB1 data could constrain  $H_0$  to 1% precision in all the IDE models, which is tighter than the corresponding results from the CMB+BAO+SN data.

We also treat the DM parameters as free parameters to study the effects of the correlations between them and cosmological parameters. Jointly constraining the FRB properties and cosmological parameters would increase the constraint errors of  $\beta$  by a factor of about 0.5–2. In this work, we use the Macquart relation to constrain the IDE models at the background level. A future work could use auto-correlations of FRBs and cross-correlations with the large-scale structure to constrain cosmological parameters with clustering effects [111–114].

## Acknowledgments

We thank Jing-Zhao Qi, Hai-Li Li, and Yichao Li for helpful discussions. This work was supported by the National SKA Program of China (Grants Nos. 2022SKA0110200 and

2022SKA0110203) and the National Natural Science Foundation of China (Grants Nos. 11975072, 11835009, and 11875102).

## References

- [1] CHIME/FRB collaboration, *A bright millisecond-duration radio burst from a Galactic magnetar*, *Nature* **587** (2020) 54 [2005.10324].
- [2] C.D. Bochenek, V. Ravi, K.V. Belov, G. Hallinan, J. Kocz, S.R. Kulkarni et al., *A fast radio burst associated with a Galactic magnetar*, *Nature* **587** (2020) 59 [2005.10828].
- [3] J.P. Macquart et al., *A census of baryons in the Universe from localized fast radio bursts*, *Nature* **581** (2020) 391 [2005.13161].
- [4] W. Deng and B. Zhang, *Cosmological Implications of Fast Radio Burst/Gamma-Ray Burst Associations*, *Astrophys. J. Lett.* **783** (2014) L35 [1401.0059].
- [5] H. Gao, Z. Li and B. Zhang, *Fast Radio Burst/Gamma-Ray Burst Cosmography*, *Astrophys. J.* **788** (2014) 189 [1402.2498].
- [6] B. Zhou, X. Li, T. Wang, Y.-Z. Fan and D.-M. Wei, *Fast radio bursts as a cosmic probe?*, *Phys. Rev. D* **89** (2014) 107303 [1401.2927].
- [7] Y.-P. Yang and B. Zhang, *Extracting host galaxy dispersion measure and constraining cosmological parameters using fast radio burst data*, *Astrophys. J. Lett.* **830** (2016) L31 [1608.08154].
- [8] Z.-X. Li, H. Gao, X.-H. Ding, G.-J. Wang and B. Zhang, *Strongly lensed repeating fast radio bursts as precision probes of the universe*, *Nature Commun.* **9** (2018) 3833 [1708.06357].
- [9] A. Walters, A. Weltman, B.M. Gaensler, Y.-Z. Ma and A. Witzemann, *Future Cosmological Constraints from Fast Radio Bursts*, *Astrophys. J.* **856** (2018) 65 [1711.11277].
- [10] M. Jaroszynski, *Fast Radio Bursts and cosmological tests*, *Mon. Not. Roy. Astron. Soc.* **484** (2019) 1637 [1812.11936].
- [11] B. Liu, Z. Li, H. Gao and Z.-H. Zhu, *Prospects of strongly lensed repeating fast radio bursts: Complementary constraints on dark energy evolution*, *Phys. Rev. D* **99** (2019) 123517 [1907.10488].
- [12] T. Liu, S. Cao, J. Zhang, S. Geng, Y. Liu, X. Ji et al., *Implications from simulated strong gravitational lensing systems: constraining cosmological parameters using Gaussian Processes*, *Astrophys. J.* **886** (2019) 94 [1910.02592].
- [13] L. Zhang and Z. Li, *Combinations of Standard Pings and Standard Candles: An Effective and Hubble Constant-free Probe of Dark Energy Evolution*, *Astrophys. J.* **901** (2020) 130.
- [14] D.-C. Qiang and H. Wei, *Effect of Redshift Distributions of Fast Radio Bursts on Cosmological Constraints*, *Phys. Rev. D* **103** (2021) 083536 [2102.00579].
- [15] J.-P. Dai and J.-Q. Xia, *Reconstruction of baryon fraction in intergalactic medium through dispersion measurements of fast radio bursts*, *Mon. Not. Roy. Astron. Soc.* **503** (2021) 4576 [2103.08479].
- [16] S. Zhao, B. Liu, Z. Li and H. Gao, *Model-independent Estimation of  $H_0$  and  $\Omega_K$  from Strongly Lensed Fast Radio Bursts*, *Astrophys. J.* **916** (2021) 70.
- [17] C. Zhu and J. Zhang, *Improvement of cosmological constraints with the cross-correlation between line-of-sight optical galaxy and FRB dispersion measures*, *Phys. Rev. D* **106** (2022) 023513 [2205.03867].
- [18] P.-J. Wu, Y. Shao, S.-J. Jin and X. Zhang, *A path to precision cosmology: Synergy between four promising late-universe cosmological probes*, 2202.09726.

- [19] Z. Li, H. Gao, J.-J. Wei, Y.-P. Yang, B. Zhang and Z.-H. Zhu, *Cosmology-independent estimate of the fraction of baryon mass in the IGM from fast radio burst observations*, *Astrophys. J.* **876** (2019) 146 [[1904.08927](#)].
- [20] J.-J. Wei, Z. Li, H. Gao and X.-F. Wu, *Constraining the Evolution of the Baryon Fraction in the IGM with FRB and  $H(z)$  data*, *JCAP* **09** (2019) 039 [[1907.09772](#)].
- [21] Q. Wu, H. Yu and F.Y. Wang, *A New Method to Measure Hubble Parameter  $H(z)$  using Fast Radio Bursts*, *Astrophys. J.* **895** (2020) 33 [[2004.12649](#)].
- [22] K.-G. Lee, M. Ata, I.S. Khrykin, Y. Huang, J.X. Prochaska, J. Cooke et al., *Constraining the Cosmic Baryon Distribution with Fast Radio Burst Foreground Mapping*, *Astrophys. J.* **928** (2022) 9 [[2109.00386](#)].
- [23] R. Gao, Z. Li and H. Gao, *Prospects of strongly lensed fast radio bursts: simultaneous measurement of post-Newtonian parameter and Hubble constant*, *Mon. Not. Roy. Astron. Soc.* **516** (2022) 1977 [[2208.10175](#)].
- [24] R. Reischke and S. Hagstotz, *Consistent Constraints on the Equivalence Principle from localised Fast Radio Bursts*, [2302.10072](#).
- [25] S. Bhandari and C. Flynn, *Probing the Universe with Fast Radio Bursts*, *Universe* **7** (2021) 85.
- [26] D. Xiao, F. Wang and Z. Dai, *The physics of fast radio bursts*, *Sci. China Phys. Mech. Astron.* **64** (2021) 249501 [[2101.04907](#)].
- [27] E. Petroff, J.W.T. Hessels and D.R. Lorimer, *Fast radio bursts at the dawn of the 2020s*, *Astron. Astrophys. Rev.* **30** (2022) 2 [[2107.10113](#)].
- [28] M. Caleb and E. Keane, *A Decade and a Half of Fast Radio Burst Observations*, *Universe* **7** (2021) 453.
- [29] CHIME/FRB collaboration, *The First CHIME/FRB Fast Radio Burst Catalog*, *Astrophys. J. Supp.* **257** (2021) 59 [[2106.04352](#)].
- [30] S. Hagstotz, R. Reischke and R. Lilow, *A new measurement of the Hubble constant using fast radio bursts*, *Mon. Not. Roy. Astron. Soc.* **511** (2022) 662 [[2104.04538](#)].
- [31] Q. Wu, G.-Q. Zhang and F.-Y. Wang, *An 8 per cent determination of the Hubble constant from localized fast radio bursts*, *Mon. Not. Roy. Astron. Soc.* **515** (2022) L1 [[2108.00581](#)].
- [32] C.W. James et al., *A measurement of Hubble's Constant using Fast Radio Bursts*, [2208.00819](#).
- [33] Y. Liu, H. Yu and P. Wu, *Cosmological-model-independent determination of Hubble constant from fast radio bursts and Hubble parameter measurements*, [2210.05202](#).
- [34] Z.-W. Zhao, J.-G. Zhang, Y. Li, J.-M. Zou, J.-F. Zhang and X. Zhang, *First statistical measurement of the Hubble constant using unlocalized fast radio bursts*, [2212.13433](#).
- [35] Z.-W. Zhao, Z.-X. Li, J.-Z. Qi, H. Gao, J.-F. Zhang and X. Zhang, *Cosmological parameter estimation for dynamical dark energy models with future fast radio burst observations*, *Astrophys. J.* **903** (2020) 83 [[2006.01450](#)].
- [36] X.-W. Qiu, Z.-W. Zhao, L.-F. Wang, J.-F. Zhang and X. Zhang, *A forecast of using fast radio burst observations to constrain holographic dark energy*, *JCAP* **02** (2022) 006 [[2108.04127](#)].
- [37] B. Wang, E. Abdalla, F. Atrio-Barandela and D. Pavon, *Dark Matter and Dark Energy Interactions: Theoretical Challenges, Cosmological Implications and Observational Signatures*, *Rept. Prog. Phys.* **79** (2016) 096901 [[1603.08299](#)].
- [38] D. Comelli, M. Pietroni and A. Riotto, *Dark energy and dark matter*, *Phys. Lett. B* **571** (2003) 115 [[hep-ph/0302080](#)].

- [39] R.-G. Cai and A. Wang, *Cosmology with interaction between phantom dark energy and dark matter and the coincidence problem*, *JCAP* **03** (2005) 002 [[hep-th/0411025](#)].
- [40] X. Zhang, *Coupled quintessence in a power-law case and the cosmic coincidence problem*, *Mod. Phys. Lett. A* **20** (2005) 2575 [[astro-ph/0503072](#)].
- [41] J.-H. He and B. Wang, *Effects of the interaction between dark energy and dark matter on cosmological parameters*, *JCAP* **06** (2008) 010 [[0801.4233](#)].
- [42] J.-H. He, B. Wang and P. Zhang, *The Imprint of the interaction between dark sectors in large scale cosmic microwave background anisotropies*, *Phys. Rev. D* **80** (2009) 063530 [[0906.0677](#)].
- [43] E. Di Valentino, A. Melchiorri and O. Mena, *Can interacting dark energy solve the  $H_0$  tension?*, *Phys. Rev. D* **96** (2017) 043503 [[1704.08342](#)].
- [44] W. Yang, S. Pan, E. Di Valentino, R.C. Nunes, S. Vagnozzi and D.F. Mota, *Tale of stable interacting dark energy, observational signatures, and the  $H_0$  tension*, *JCAP* **09** (2018) 019 [[1805.08252](#)].
- [45] W. Yang, A. Mukherjee, E. Di Valentino and S. Pan, *Interacting dark energy with time varying equation of state and the  $H_0$  tension*, *Phys. Rev. D* **98** (2018) 123527 [[1809.06883](#)].
- [46] S. Pan, W. Yang, E. Di Valentino, E.N. Saridakis and S. Chakraborty, *Interacting scenarios with dynamical dark energy: Observational constraints and alleviation of the  $H_0$  tension*, *Phys. Rev. D* **100** (2019) 103520 [[1907.07540](#)].
- [47] E. Di Valentino, A. Melchiorri, O. Mena and S. Vagnozzi, *Interacting dark energy in the early 2020s: A promising solution to the  $H_0$  and cosmic shear tensions*, *Phys. Dark Univ.* **30** (2020) 100666 [[1908.04281](#)].
- [48] E. Di Valentino, A. Melchiorri, O. Mena and S. Vagnozzi, *Nonminimal dark sector physics and cosmological tensions*, *Phys. Rev. D* **101** (2020) 063502 [[1910.09853](#)].
- [49] S. Vagnozzi, *New physics in light of the  $H_0$  tension: An alternative view*, *Phys. Rev. D* **102** (2020) 023518 [[1907.07569](#)].
- [50] L.-Y. Gao, Z.-W. Zhao, S.-S. Xue and X. Zhang, *Relieving the  $H_0$  tension with a new interacting dark energy model*, *JCAP* **07** (2021) 005 [[2101.10714](#)].
- [51] J. Zhang, H. Liu and X. Zhang, *Statefinder diagnosis for the interacting model of holographic dark energy*, *Phys. Lett. B* **659** (2008) 26 [[0705.4145](#)].
- [52] L. Zhang, J. Cui, J. Zhang and X. Zhang, *Interacting model of new agegraphic dark energy: Cosmological evolution and statefinder diagnostic*, *Int. J. Mod. Phys. D* **19** (2010) 21 [[0911.2838](#)].
- [53] M. Li, X.-D. Li, S. Wang, Y. Wang and X. Zhang, *Probing interaction and spatial curvature in the holographic dark energy model*, *JCAP* **12** (2009) 014 [[0910.3855](#)].
- [54] Y. Li, J. Ma, J. Cui, Z. Wang and X. Zhang, *Interacting model of new agegraphic dark energy: observational constraints and age problem*, *Sci. China Phys. Mech. Astron.* **54** (2011) 1367 [[1011.6122](#)].
- [55] Y.-H. Li and X. Zhang, *Running coupling: Does the coupling between dark energy and dark matter change sign during the cosmological evolution?*, *Eur. Phys. J. C* **71** (2011) 1700 [[1103.3185](#)].
- [56] Z. Zhang, S. Li, X.-D. Li, X. Zhang and M. Li, *Revisit of the Interaction between Holographic Dark Energy and Dark Matter*, *JCAP* **06** (2012) 009 [[1204.6135](#)].
- [57] J. Zhang, L. Zhao and X. Zhang, *Revisiting the interacting model of new agegraphic dark energy*, *Sci. China Phys. Mech. Astron.* **57** (2014) 387 [[1306.1289](#)].
- [58] Y.-H. Li and X. Zhang, *Large-scale stable interacting dark energy model: Cosmological perturbations and observational constraints*, *Phys. Rev. D* **89** (2014) 083009 [[1312.6328](#)].

- [59] Y.-H. Li, J.-F. Zhang and X. Zhang, *Parametrized Post-Friedmann Framework for Interacting Dark Energy*, *Phys. Rev. D* **90** (2014) 063005 [[1404.5220](#)].
- [60] Y.-H. Li, J.-F. Zhang and X. Zhang, *Exploring the full parameter space for an interacting dark energy model with recent observations including redshift-space distortions: Application of the parametrized post-Friedmann approach*, *Phys. Rev. D* **90** (2014) 123007 [[1409.7205](#)].
- [61] J.-J. Geng, Y.-H. Li, J.-F. Zhang and X. Zhang, *Redshift drift exploration for interacting dark energy*, *Eur. Phys. J. C* **75** (2015) 356 [[1501.03874](#)].
- [62] Y.-H. Li, J.-F. Zhang and X. Zhang, *Testing models of vacuum energy interacting with cold dark matter*, *Phys. Rev. D* **93** (2016) 023002 [[1506.06349](#)].
- [63] L. Amendola, *Scaling solutions in general nonminimal coupling theories*, *Phys. Rev. D* **60** (1999) 043501 [[astro-ph/9904120](#)].
- [64] A.P. Billyard and A.A. Coley, *Interactions in scalar field cosmology*, *Phys. Rev. D* **61** (2000) 083503 [[astro-ph/9908224](#)].
- [65] Z.-K. Guo, N. Ohta and S. Tsujikawa, *Probing the Coupling between Dark Components of the Universe*, *Phys. Rev. D* **76** (2007) 023508 [[astro-ph/0702015](#)].
- [66] J.-Q. Xia, *Constraint on coupled dark energy models from observations*, *Phys. Rev. D* **80** (2009) 103514 [[0911.4820](#)].
- [67] J.-H. He, B. Wang and E. Abdalla, *Testing the interaction between dark energy and dark matter via latest observations*, *Phys. Rev. D* **83** (2011) 063515 [[1012.3904](#)].
- [68] T.-F. Fu, J.-F. Zhang, J.-Q. Chen and X. Zhang, *Holographic Ricci dark energy: Interacting model and cosmological constraints*, *Eur. Phys. J. C* **72** (2012) 1932 [[1112.2350](#)].
- [69] R. Murgia, S. Gariazzo and N. Fornengo, *Constraints on the Coupling between Dark Energy and Dark Matter from CMB data*, *JCAP* **04** (2016) 014 [[1602.01765](#)].
- [70] A.A. Costa, X.-D. Xu, B. Wang and E. Abdalla, *Constraints on interacting dark energy models from Planck 2015 and redshift-space distortion data*, *JCAP* **01** (2017) 028 [[1605.04138](#)].
- [71] L. Feng and X. Zhang, *Revisit of the interacting holographic dark energy model after Planck 2015*, *JCAP* **08** (2016) 072 [[1607.05567](#)].
- [72] D.-M. Xia and S. Wang, *Constraining interacting dark energy models with latest cosmological observations*, *Mon. Not. Roy. Astron. Soc.* **463** (2016) 952 [[1608.04545](#)].
- [73] R.-Y. Guo, J.-F. Zhang and X. Zhang, *Exploring neutrino mass and mass hierarchy in the scenario of vacuum energy interacting with cold dark matter*, *Chin. Phys. C* **42** (2018) 095103 [[1803.06910](#)].
- [74] H.-L. Li, L. Feng, J.-F. Zhang and X. Zhang, *Models of vacuum energy interacting with cold dark matter: Constraints and comparison*, *Sci. China Phys. Mech. Astron.* **62** (2019) 120411 [[1812.00319](#)].
- [75] L. Feng, D.-Z. He, H.-L. Li, J.-F. Zhang and X. Zhang, *Constraints on active and sterile neutrinos in an interacting dark energy cosmology*, *Sci. China Phys. Mech. Astron.* **63** (2020) 290404 [[1910.03872](#)].
- [76] G. Cheng, Y.-Z. Ma, F. Wu, J. Zhang and X. Chen, *Testing interacting dark matter and dark energy model with cosmological data*, *Phys. Rev. D* **102** (2020) 043517 [[1911.04520](#)].
- [77] M. Aljaf, D. Gregoris and M. Khurshudyan, *Constraints on interacting dark energy models through cosmic chronometers and Gaussian process*, *Eur. Phys. J. C* **81** (2021) 544 [[2005.01891](#)].

- [78] H.-L. Li, J.-F. Zhang and X. Zhang, *Constraints on neutrino mass in the scenario of vacuum energy interacting with cold dark matter after Planck 2018*, *Commun. Theor. Phys.* **72** (2020) 125401 [2005.12041].
- [79] M. Zhang, B. Wang, P.-J. Wu, J.-Z. Qi, Y. Xu, J.-F. Zhang et al., *Prospects for Constraining Interacting Dark Energy Models with 21 cm Intensity Mapping Experiments*, *Astrophys. J.* **918** (2021) 56 [2102.03979].
- [80] M. Lucca, *Multi-interacting dark energy and its cosmological implications*, *Phys. Rev. D* **104** (2021) 083510 [2106.15196].
- [81] R.C. Nunes, S. Vagnozzi, S. Kumar, E. Di Valentino and O. Mena, *New tests of dark sector interactions from the full-shape galaxy power spectrum*, *Phys. Rev. D* **105** (2022) 123506 [2203.08093].
- [82] W. Yang, S. Pan, E. Di Valentino, O. Mena and A. Melchiorri, *2021-H0 odyssey: closed, phantom and interacting dark energy cosmologies*, *JCAP* **10** (2021) 008 [2101.03129].
- [83] R.-Y. Guo, L. Feng, T.-Y. Yao and X.-Y. Chen, *Exploration of interacting dynamical dark energy model with interaction term including the equation-of-state parameter: alleviation of the  $H_0$  tension*, *JCAP* **12** (2021) 036 [2110.02536].
- [84] L.-F. Wang, J.-H. Zhang, D.-Z. He, J.-F. Zhang and X. Zhang, *Constraints on interacting dark energy models from time-delay cosmography with seven lensed quasars*, *Mon. Not. Roy. Astron. Soc.* **514** (2022) 1433 [2102.09331].
- [85] S.-J. Jin, R.-Q. Zhu, L.-F. Wang, H.-L. Li, J.-F. Zhang and X. Zhang, *Impacts of gravitational-wave standard siren observations from Einstein Telescope and Cosmic Explorer on weighing neutrinos in interacting dark energy models*, *Commun. Theor. Phys.* **74** (2022) 105404 [2204.04689].
- [86] E. Majerotto, J. Valiviita and R. Maartens, *Instability in interacting dark energy and dark matter fluids*, *Nucl. Phys. B Proc. Suppl.* **194** (2009) 260.
- [87] T. Clemson, K. Koyama, G.-B. Zhao, R. Maartens and J. Valiviita, *Interacting Dark Energy – constraints and degeneracies*, *Phys. Rev. D* **85** (2012) 043007 [1109.6234].
- [88] J.-H. He, B. Wang and E. Abdalla, *Stability of the curvature perturbation in dark sectors’ mutual interacting models*, *Phys. Lett. B* **671** (2009) 139 [0807.3471].
- [89] W. Fang, W. Hu and A. Lewis, *Crossing the Phantom Divide with Parameterized Post-Friedmann Dark Energy*, *Phys. Rev. D* **78** (2008) 087303 [0808.3125].
- [90] W. Hu, *Parameterized Post-Friedmann Signatures of Acceleration in the CMB*, *Phys. Rev. D* **77** (2008) 103524 [0801.2433].
- [91] X. Zhang, *Probing the interaction between dark energy and dark matter with the parameterized post-Friedmann approach*, *Sci. China Phys. Mech. Astron.* **60** (2017) 050431 [1702.04564].
- [92] L. Feng, Y.-H. Li, F. Yu, J.-F. Zhang and X. Zhang, *Exploring interacting holographic dark energy in a perturbed universe with parameterized post-Friedmann approach*, *Eur. Phys. J. C* **78** (2018) 865 [1807.03022].
- [93] J.M. Shull, B.D. Smith and C.W. Danforth, *The Baryon Census in a Multiphase Intergalactic Medium: 30% of the Baryons May Still Be Missing*, *Astrophys. J.* **759** (2012) 23 [1112.2706].
- [94] X.-H. Fan, C.L. Carilli and B.G. Keating, *Observational constraints on cosmic reionization*, *Ann. Rev. Astron. Astrophys.* **44** (2006) 415 [astro-ph/0602375].
- [95] M. McQuinn, *Locating the “missing” baryons with extragalactic dispersion measure estimates*, *Astrophys. J. Lett.* **780** (2014) L33 [1309.4451].
- [96] R. Reischke and S. Hagstotz, *Covariance Matrix of Fast Radio Bursts Dispersion*, 2301.03527.

- [97] G.Q. Zhang, H. Yu, J.H. He and F.Y. Wang, *Dispersion measures of fast radio burst host galaxies derived from IllustrisTNG simulation*, *Astrophys. J.* **900** (2020) 170 [2007.13935].
- [98] T. Hashimoto, T. Goto, A.Y.L. On, T.-Y. Lu, D.J.D. Santos, S.C.C. Ho et al., *Fast radio bursts to be detected with the Square Kilometre Array*, *Mon. Not. Roy. Astron. Soc.* **497** (2020) 4107 [2008.00007].
- [99] J.-G. Zhang, Z.-W. Zhao, Y.-C. Li, J.-F. Zhang, D. Li and X. Zhang, *Cosmology with fast radio bursts in the era of SKA, in preparation*.
- [100] R.C. Zhang and B. Zhang, *The CHIME Fast Radio Burst Population Does Not Track the Star Formation History of the Universe*, *Astrophys. J. Lett.* **924** (2022) L14 [2109.07558].
- [101] D.-C. Qiang, S.-L. Li and H. Wei, *Fast radio burst distributions consistent with the first CHIME/FRB catalog*, *JCAP* **01** (2022) 040 [2111.07476].
- [102] P. Madau and T. Fragos, *Radiation Backgrounds at Cosmic Dawn: X-Rays from Compact Binaries*, *Astrophys. J.* **840** (2017) 39 [1606.07887].
- [103] L. Chen, Q.-G. Huang and K. Wang, *Distance Priors from Planck Final Release*, *JCAP* **02** (2019) 028 [1808.05724].
- [104] F. Beutler, C. Blake, M. Colless, D.H. Jones, L. Staveley-Smith, L. Campbell et al., *The 6dF Galaxy Survey: Baryon Acoustic Oscillations and the Local Hubble Constant*, *Mon. Not. Roy. Astron. Soc.* **416** (2011) 3017 [1106.3366].
- [105] A.J. Ross, L. Samushia, C. Howlett, W.J. Percival, A. Burden and M. Manera, *The clustering of the SDSS DR7 main Galaxy sample – I. A 4 per cent distance measure at  $z = 0.15$* , *Mon. Not. Roy. Astron. Soc.* **449** (2015) 835 [1409.3242].
- [106] BOSS collaboration, *The clustering of galaxies in the completed SDSS-III Baryon Oscillation Spectroscopic Survey: cosmological analysis of the DR12 galaxy sample*, *Mon. Not. Roy. Astron. Soc.* **470** (2017) 2617 [1607.03155].
- [107] PAN-STARRS1 collaboration, *The Complete Light-curve Sample of Spectroscopically Confirmed SNe Ia from Pan-STARRS1 and Cosmological Constraints from the Combined Pantheon Sample*, *Astrophys. J.* **859** (2018) 101 [1710.00845].
- [108] A. Lewis, A. Challinor and A. Lasenby, *Efficient computation of CMB anisotropies in closed FRW models*, *Astrophys. J.* **538** (2000) 473 [astro-ph/9911177].
- [109] A. Lewis and S. Bridle, *Cosmological parameters from CMB and other data: A Monte Carlo approach*, *Phys. Rev. D* **66** (2002) 103511 [astro-ph/0205436].
- [110] S. Koch Ocker et al., *The Large Dispersion and Scattering of FRB 20190520B Are Dominated by the Host Galaxy*, *Astrophys. J.* **931** (2022) 87 [2202.13458].
- [111] K.W. Masui and K. Sigurdson, *Dispersion Distance and the Matter Distribution of the Universe in Dispersion Space*, *Phys. Rev. Lett.* **115** (2015) 121301 [1506.01704].
- [112] R. Reischke, S. Hagstotz and R. Lilow, *Probing primordial non-Gaussianity with Fast Radio Bursts*, *Phys. Rev. D* **103** (2021) 023517 [2007.04054].
- [113] M. Shirasaki, R. Takahashi, K. Osato and K. Ioka, *Probing cosmology and astrophysics with fast radio bursts: cross-correlations of dark matter haloes and cosmic dispersion measures*, *Mon. Not. Roy. Astron. Soc.* **512** (2022) 1730 [2108.12205].
- [114] M. Rafiei-Ravandi et al., *CHIME/FRB Catalog 1 Results: Statistical Cross-correlations with Large-scale Structure*, *Astrophys. J.* **922** (2021) 42 [2106.04354].